Feedback from Massive YSOs and Massive Stars

You-Hua Chu[1] and Robert A. Gruendl[1]

[1] Astronomy Department, University of Illinois, Urbana, IL 61801, USA

Abstract: Massive stars are powerful sources of radiation, stellar winds, and supernova explosions. The radiative and mechanical energies injected by massive stars into the interstellar medium (ISM) profoundly alter the structure and evolution of the ISM, which subsequently influences the star formation and chemical evolution of the host galaxy. In this review, we will use the Large Magellanic Cloud (LMC) as a laboratory to showcase effects of energy feedback from massive young stellar objects (YSOs) and mature stars. We will also use the Carina Nebula in the Galaxy to illustrate a multi-wavelength study of feedback from massive star.

1   Introduction

Massive stars generate large amounts of energy and are thus luminous. The energy leaves a star mainly in the form of radiation; only a small portion of the energy is imparted to the stellar wind through line scattering. For example, an O5 main sequence star has a luminosity of $\sim 10^6 \ L_\odot$, or $\sim 4 \times 10^{39}$ ergs s^{-1}, while the mechanical luminosity of its stellar wind is only $L_w \sim 1.3 \times 10^{35}$ ergs s^{-1}, assuming a typical mass loss rate ($\dot{M}$) of 10^{-7} M$_\odot$ yr^{-1} and a wind terminal velocity (V_w) of 2000 km s^{-1}. As a massive star evolves and traces a nearly horizontal track in the theoretical HR diagram, its luminosity is nearly constant, but its varying effective temperature leads to different mass loss rates and stellar wind velocities. For example, a red supergiant has a higher $\dot{M}$, $\sim 10^{-4}$ M$_\odot$ yr^{-1}, but a lower V_w, 10–50 km s^{-1}, and its L_w is even lower, $\sim 10^{34}$ ergs s^{-1}. A Wolf-Rayet (WR) star, on the other hand, has both a high $\dot{M}$ and a high V_w, and thus the highest L_w, 10^{37}–10^{38} ergs s^{-1}, which is still much lower than its luminosity.

At infancy, the radiation of a massive young stellar object (YSO) can heat and repel the ambient dust, photo-dissociate molecules, and photo-ionize atoms, while its stellar wind clears out the circumstellar material and further erodes the placental molecular cloud. During its adulthood, a massive star's radiation photo-ionizes and heats its ambient interstellar medium (ISM) to 10^4 K, and its stellar wind dynamically interacts with the ISM, blowing bubbles and generating turbulence. At the end of its life, a massive star explodes as a supernova, releasing $\sim 10^{51}$ ergs of kinetic energy into the ISM, forming a classical supernova remnant (SNR) in a dense medium, or merely heating its ambient medium further if it is in a hot low-density medium such as the interior of a superbubble.

Stellar energy feedback profoundly alters the structure of the ISM by producing interstellar shells up to 10^3 pc in size, injecting turbulence, creating multiple phase components with different physical conditions, and ejecting hot gas into the galactic halo. As stars are formed from the ISM, the physical changes of the ISM affect the future generation of star formation, either dispersing or compressing

the ISM to inhibit or enhance star formation. The mass loss from massive stars enriches the ISM and the intergalactic medium, contributing to the chemical evolution of a galaxy.

Sites of stellar energy feedback provide excellent laboratories for us to study a wide range of astrophysical processes, such as shocks, thermal conduction, turbulence, cosmic ray acceleration, etc. Observations of stellar energy feedback allow us to better grasp its ramifications on cosmic evolution. It is thus important to study stellar energy feedback. Unlike star formation, however, there is no simple recipe for stellar energy feedback because the ISM surrounding massive stars has diverse physical conditions, resulting in complex dynamical interactions.

2   The Large Magellanic Cloud as a Laboratory

The actions of energy feedback from massive stars are best observed in a galaxy where a clear, high-resolution view of both stars and the ISM for the entire galaxy can be obtained. The Large Magellanic Cloud (LMC) provides such an ideal laboratory to study massive stars acting on the ISM because of its nearly face-on orientation, small distance (50 kpc, where $1''$ corresponds to 0.25 pc), and low foreground extinction.

The LMC has been surveyed extensively for both stars and the ISM: $UBVI$ photometry of bright stars (MCPS, Zaritsky et al. 2004), emission-line survey of ionized gas (MCELS, Smith and the MCELS Team 1999), *ROSAT* X-ray mosaic image of the hot (10^6 K) ionized gas (made by S. Snowden), ATCA+Parkes 21-cm line survey of H I (Kim et al. 2003), *Spitzer* near- and mid-IR surveys of stars and dust (SAGE, Meixner et al. 2006), and CO surveys of molecular clouds (NANTEN, Fukui et al. 2008; MAGMA, Hughes et al. 2010). These surveys provide a detailed view of the distributions, physical conditions, and kinematics of the ISM and the underlying stellar population in the LMC.

Figure 1 displays some of the survey images to illustrate the full view of the LMC at different wavelengths: MCPS optical continuum, 2MASS K-band, *Spitzer* IRAC and MIPS composite, MCELS Hα, *ROSAT* PSPC mosaic in the 0.5–2.0 keV band, and ATCA+Parkes H I 21 cm line. These detailed surveys of stars and ISM enable many studies that are not possible in the Galaxy or in more distant galaxies. For example:

- The MCPS data have been used to determine the spatially-resolved star formation history of the LMC (Harris & Zaritsky 2009), and this star formation history combined with Starburst99 (Leitherer et al. 1999) can be used to estimate the history of stellar energy injected into the ISM.

- The actual stellar content of a superbubble can be observed to estimate the total stellar energy input, and the kinetic energy in the expanding shell and the thermal energy in the superbubble interior can be measured to determine the stellar energy retained in the ISM. It is found that the ISM retains much less energy than the total stellar energy injected (Cooper et al. 2004).

- The *Spitzer* survey of the LMC can be used to search for stars with IR excesses indicating circumstellar dust and to identify YSOs (Gruendl & Chu 2009). The power spectrum analysis of *Spitzer* images shows two power laws with different slopes joining at a scale of 100–200 pc, which may be a scale height of the dust disk of the LMC (Puerari et al. 2010).

- The stellar mass distribution assessed from the 2MASS survey and the gas distribution derived from the H I and CO surveys can be used to determine the gravitational instability map of the LMC, and it is found that ∼85% of the massive YSOs are located within the unstable regions (Yang et al. 2007).

- Star formation related to stellar energy feedback can be studied in detail around OB associations and superbubbles (Chen et al. 2009, 2010) as well as supergiant shells (Book et al. 2009).
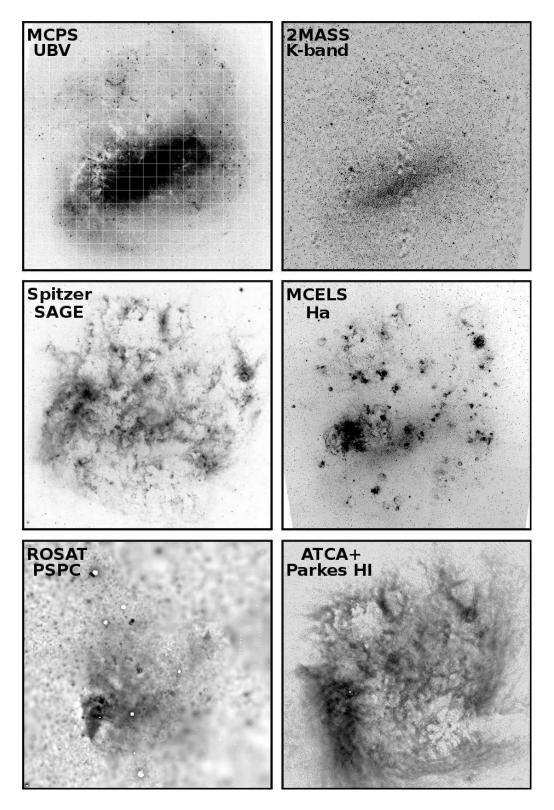
Figure 1: Multi-wavelength images of the LMC. The top row displays the MCPS composite image from Harris & Zaritsky (2009) and 2MASS K-band image, the middle row the *Spitzer* SAGE composite image from Meixner et al. (2006) and MCELS Hα image from Smith & the MCELS Team (1999), and the bottom row the *ROSAT* PSPC mosaic in the 0.5–2.0 keV band made by S. Snowden and ATCA+Parkes H I map from Kim et al. (2003). Note that these images do not have identical scales and orientation.
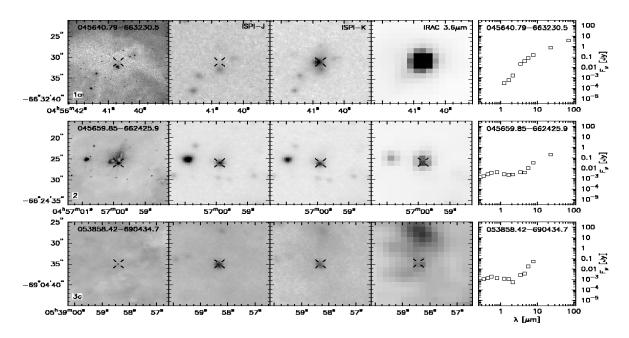
Figure 2: Images and SEDs of three YSOs with three different types of immediate environments: in a dark cloud (top row), in the tip of a bright-rimmed dust pillar (middle row), and in a small H II region (bottom row). The images from left to right are: *HST* Hα, CTIO 4m ISPI J and K, *Spitzer* IRAC 3.6 μm. The rightmost panel shows the SED.

It is impossible to review every stellar energy feedback topic. In this paper, we have selected a few obvious topics in which recent progress has been made: (1) dispersal of molecular clouds, (2) interstellar shells, (3) acceleration of cosmic rays, and (4) anatomy of the Carina Nebula.

3   Massive Star Formation and Dispersal of Molecular Clouds

To investigate the energy feedback of massive stars in their infancy, we can examine the immediate surroundings of massive YSOs. A large sample of massive and intermediate-mass YSOs have been identified in the LMC (Gruendl & Chu 2009). About 100 of these YSOs have archival *Hubble Space Telescope* (*HST*) Hα and continuum images available. These Hα images reveal three types of immediate environments of YSOs: in dark clouds, inside or on the tip of bright-rimmed dust pillars, and in small H II regions (Vaidya et al. 2009). Figure 2 shows images and spectral energy distributions (SEDs) of three exemplary YSOs. It is suggested that the three types of environments represent an evolutionary sequence, as the stellar wind clears out the ambient molecular cloud and reveals a small H II region. This evolutionary sequence is supported by the evolutionary stages of the YSOs indicated by their SEDs.

The dispersal of ambient molecular material by massive YSOs is also seen in direct observations of HCO^+, a tracer for dense molecular gas. Using the ATCA facility, HCO^+ has been mapped in two OB/H II complexes: N44 (Seale et al., in preparation) and N159 (Chen et al., in preparation). Many YSOs in these two complexes have *Spitzer* IRS spectra available. Based on the progressive presence of silicate absorption, PAH emission, and fine-structure atomic line emission, an evolutionary sequence of YSOs can be defined (Seale et al. 2009). It is observed that the youngest YSOs, those with silicate absorption, are still coincident with molecular cores indicated by HCO^+ peaks, while the intermediate-aged YSOs show offsets from molecular cores, and the most evolved YSOs are no longer associated with molecular cores. Both the aforementioned *HST* Hα observations and these HCO^+ observations suggest that massive YSOs quickly disperse their ambient molecular material,
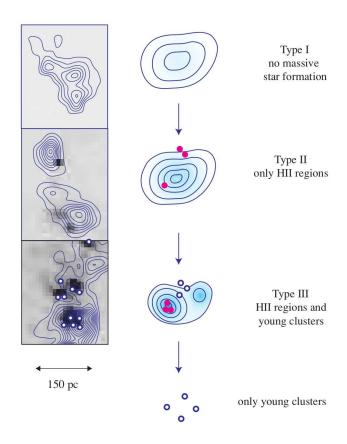
Figure 3: Evolutionary sequence of molecular clouds from Kawamura et al. (2009).

probably before they reach the main sequence.

On a larger scale, the dispersal of molecular clouds in the LMC has been studied by Kawamura et al. (2009). They find three types of molecular clouds: Type I has no massive star formation, as indicated by a lack of Hα emission; Type II has isolated massive star formation, as indicated by small discrete H II regions; and Type III has young clusters and prominent H II regions (see Figure 3). As 66% of LMC clusters younger than 10 Myr are associated with molecular clouds, Type III molecular clouds probably last for $\sim$7 Myr. If the three types of molecular clouds form an evolutionary sequence and the relative population of these three types is proportional to the time spent in these stages, then the population ratio of $N_I : N_{II} : N_{III} =$ 1: 2 :1 implies that the dispersal timescale of molecular clouds is $\sim$30 Myr.

4 Energy Feedback and Interstellar Shells

To study the energy feedback from massive stars, one ought to bear in mind that both stars and the ISM evolve, and that their evolutions are always intertwined, especially for a system like an OB association or a cluster. From birth to a few Myr old, massive O stars photo-ionize the ambient ISM to form an H II region. Starting at $\sim$5 Myr, O stars start to explode as supernovae. The combined action of fast stellar winds and supernova blasts sweeps the H II region into an expanding shell, i.e., a superbubble. At $\sim$10 Myr, O stars are gone and B stars start to explode as supernovae. Without ionizing sources, the superbubble recombines and becomes an H I shell. After $\sim$15 Myr, all massive stars are gone; the remaining lower-mass stars disperse, and the H I supershell coasts along. If the superbubble is not near dense molecular material, it will have a simple shell structure, such as N70. If the superbubble is in a molecular gas-rich environment, the expanding superbubble can compress
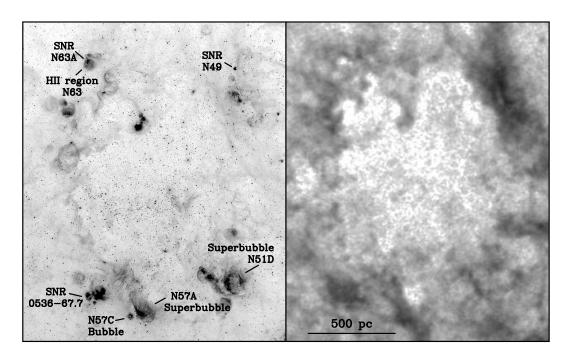
Figure 4: Hα image (left panel) and H I column density map (right panel) of supergiant shell LMC4 in the LMC. The two images have the same field-of-view. Superbubbles, SNRs, and a bubble are marked in the figure.

the ambient molecular clouds to form more stars along the shell rim, such as N11 and N44. Such sequential star formation can continue for more than 10^7 yr to form a supergiant shell reaching 1000 pc in size.

The most common product of stellar energy feedback is interstellar shells of various sizes, as illustrated in Figure 4. An isolated single massive star with a fast stellar wind can form an interstellar bubble during its main sequence stage, a circumstellar bubble (consisting of stellar material previously lost via a slow wind) during the WR star stage, and a SNR after its final explosion. The sizes of bubbles and SNRs can grow up to a few 10's of pc before dissipating and merging into the ISM. OB associations can blow superbubbles with sizes up to a few hundred pc. Multiple generations of propagated star formation over an extended period of time and space can form supergiant shells of sizes $\sim 10^3$ pc. The supergiant shell LMC4 in Figure 4 shows that the gas in this area has been cleared out, and that on-going star formation takes place along the supergiant shell rim where dense gas is present. As massive stars in LMC4 are concentrated in H II regions along the south and northeast rims, the bulk of gas associated with LMC4 is neutral, as seen in the H I column density map.

Studies of interstellar shells in recent years have provided answers to many puzzles, especially in the seeming lack of visible bubbles and rare detections of X-ray emission from bubbles. Massive O stars have fast stellar winds, and if an O star is in a reasonably dense ISM, it should blow an interstellar bubble (Weaver et al. 1977). However, bubbles are not commonly seen, and the Bubble Nebula is an exception rather than a rule. This "missing bubble" puzzle has been solved by studies of the young H II regions N11B and N180, where many O stars are present but no bubbles can be identified morphologically in optical images. Using high-dispersion, long-slit echelle spectra of N11B and N180, it has been shown that expanding shells are present around O stars, but the expansion velocities are only $\sim$20 km s^{-1}. Such weak shocks cannot compress the ambient medium to produce pronounced limb-brightening to be identifiable as a bubble (Nazé et al. 2001). When the central star evolves off the main sequence and loses its ionizing power, the bubble and the ambient medium will recombine. The isothermal sound speed of H I is low, and strong shocks and compression will be

produced by a bubble expanding at 20 km s^{-1}; therefore, H I bubbles are routinely detected around massive stars.

The difficulty in detecting diffuse X-ray emission from shocked stellar winds can be illustrated by the study of the Orion Nebula. The Orion Nebula hosts an O6 star (θ^1 Ori C) with a fast stellar wind, so it is expected to blow a bubble and the hot gas in the bubble interior should emit in X-rays. Diffuse X-ray emission from the Orion Nebula was first reported by Ku & Chanan (1979) using *Einstein* observations, but the diffuse emission was resolved into stars by *ROSAT* observations (Caillault, Gagné & Stauffer 1994). It was not until 2008 that the diffuse X-ray emission from shocked fast winds in the Orion Nebula was truly detected for the first time using *XMM-Newton* observations (Güdel et al. 2008). The *Spitzer* IRAC 8 μm image of the Orion Nebula region shows that the Orion cluster has blown a blister-like cavity, and the *XMM-Newton* observations show diffuse X-ray emission in the cavity, at the far end from the cluster. The plasma temperature determined from the X-ray spectral fits is $\sim 2 \times 10^6$ K. Future searches for diffuse X-ray emission from shocked stellar winds should bear in mind that IR images may be better at revealing bubble cavities in a complex environment and that shocked stellar wind may be located far away from the massive stars.

Many circumstellar bubbles blown by WR stars are known, but diffuse X-ray emission has been detected from only two – NGC 6888 and S 308. The plasma temperature of NGC 6888 is $\sim 2 \times 10^6$ K (Wrigge, Wendker & Wisotzki 1994) and S 308 $\sim 1 \times 10^6$ K (Chu et al. 2003). X-ray emission from such low plasma temperatures is extremely soft and the interstellar absorption is high for soft X-rays. The soft X-ray emission from S 308 can be detected because it is nearby and at a high galactic latitude, and thus its foreground absorption column density is low. If S 308 were in the Galactic plane and at a larger distance, it would not have been detected. Therefore, the higher interstellar absorption is responsible for the low X-ray detection rate of WR bubbles.

The biggest unanswered question is still the discrepancy between the observed bubble dynamics and theoretical predictions. Bubbles are observed to be too small or expand too slowly compared with those expected from bubble models using realistic stellar energy input. X-ray observations of WR bubbles, superbubbles, and planetary nebulae all show X-ray luminosities much lower than model predictions. The clumpiness of stellar winds can reduce the stellar mass loss rate by a factor of a few, but cannot fully remove the discrepancy between observations and model expectations. Artificially changing the heat conduction coefficient does not alleviate the discrepancy. Dynamically mixing cold nebular material with fast stellar wind (i.e., mass-loading) may lower the hot gas temperature, and thus raise the cooling rate. Recent models by Freyer, Hensler & Yorke (2003, 2006), Pittard, Dyson & Hartquist (2001), Pittard, Hartquist & Dyson (2001), and Arthur (2008) have grown more sophisticated. Detailed modelling for a specific bubble with accurate observations are needed for critical tests of bubble models.

It is worth noting that three cases of nonthermal X-ray emission from LMC superbubbles have been reported, but two of them are not confirmed by more careful analyses. *XMM-Newton* observations of N51D (Cooper et al. 2004) and *Suzaku* observations of N11 (Maddox et al. 2009) have been reported to show nonthermal diffuse X-ray emission from the superbubble interior. However, Yamaguchi, Sawada & Bamba (2010) have analyzed both *XMM-Newton* and *Suzaku* observations of N11 and N51D with a careful background subtraction, and found that neither show nonthermal X-ray emission. They conclude that 30 Dor C is the only LMC superbubble that shows bona fide nonthermal X-ray emission (Bamba et al. 2004; Yamaguchi et al. 2010).

5   Acceleration of Cosmic Rays

Cosmic rays can be accelerated in astronomical shocks (Bell 1978; Bykov 2001). While observations of some young SNRs have shown evidence of production of cosmic rays, the origin of Galactic cosmic

rays has been largely an unresolved mystery. The production and diffusion of cosmic rays can be traced by γ-rays, because collisions between interstellar protons and cosmic ray protons produce pions and each pion decays into two γ-rays. It is difficult to associate γ-ray emission with interstellar structures in the Galaxy because of the confusion in the Galactic plane. This is not a problem for the LMC because of its nearly face-on orientation.

Recently the *Fermi Gamma-Ray Space Telescope* detected γ-ray emission from the LMC, and provided the first spatially-resolved global view of γ-rays from a nearly face-on galaxy. Analyses of the first year's *Fermi* LAT observations of the LMC find (1) the brightest γ-ray emission appears to be centered near the 30 Dor giant H II region, but not its central R136 cluster; (2) fainter γ-ray emission is detected in the northern part of the LMC; (3) γ-ray emission shows little correlation with the total column density of the interstellar gas; and (4) γ-ray emission appears to be confined to massive star forming regions. These findings indicate that cosmic rays are accelerated in massive star forming regions and that the diffusion length of GeV cosmic ray protons is relatively short (Abdo et al. 2010).

The distribution of γ-ray emission can be compared with the underlying stellar and interstellar components. We have extracted the contours from the integrated >100 MeV emissivity map of the LMC (the left panel of Figure 10 of Abdo et al. 2010), assuming that all γ-rays are diffuse in origin, and plotted these contours in Figure 5 over the Hα image, H I column density map (Kim et al. 2003), *ROSAT* PSPC X-ray mosaic (made by S. Snowden), and star formation rates 6.3, 12.5, and 25 Myr ago (Harris & Zaritsky 2009).

Figure 5 shows that the >100 MeV emissivity is well correlated with the star formation within the last 6–12 Myr not only for the two γ-ray peaks, but also for the faint extension to the west. No correlation is seen for star formation at 25 Myr or earlier. Massive-star progenitors of supernovae have a lifetime ranging from a few to $\sim$15 Myr; thus, the correlation of γ-ray emissivity with the 6.3 and 12.5 Myr star formation rates indicates that supernovae play a major role in the acceleration of cosmic rays.

Less than 10% of massive stars are formed in isolation (Zinnecker & Yorke 2007) and produce classical SNRs. The great majority of massive stars are formed in groups, such as OB associations and clusters in single bursts of star formation, or star clouds in propagated star formation. OB associations and clusters a few Myr old produce superbubbles up to $\sim$200 pc across, while propagated star formation over 10^7 yr produce supergiant shells $\sim$1000 pc in size (Chu 2008). The Hα image and H I column density map of the LMC (Figure 5) indeed show superbubbles and supergiant shells in areas where the star formation rate was high within the last $\sim$12 Myr. Therefore, the γ-ray emission is also well correlated with superbubbles and supergiant shells. Within the brightest γ-ray peak, many superbubbles exist in the 30 Dor region; the second brightest γ-ray peak corresponds to the supergiant shell LMC4 whose periphery is dotted with superbubbles; and the faint western extension of diffuse γ-rays corresponds to the supergiant shell LMC8 (cataloged by Meaburn 1980).

It is not possible that uncataloged point sources, such as pulsars, contribute to the diffuse emission because the γ-ray emission is well correlated with the diffuse soft X-ray emission (Figure 5c) and *ROSAT* HRI observations have demonstrated that the diffuse X-ray emission is truly diffuse (Chu & Snowden 1998). Therefore, it may be concluded that the collective, interacting SNR shocks within superbubbles and supergiant shells produced by massive stars formed in the last $\sim$15 Myr have accelerated the cosmic rays in the LMC that are responsible for the >100 MeV γ-rays detected by *Fermi*.

6 Anatomy of the Carina Nebula

The Carina Nebula, at $\sim$2 kpc, is the nearest, most unobscured, giant H II region in our Galaxy. As a site of active star formation, it hosts the highest concentration of the earliest O stars in the Galaxy
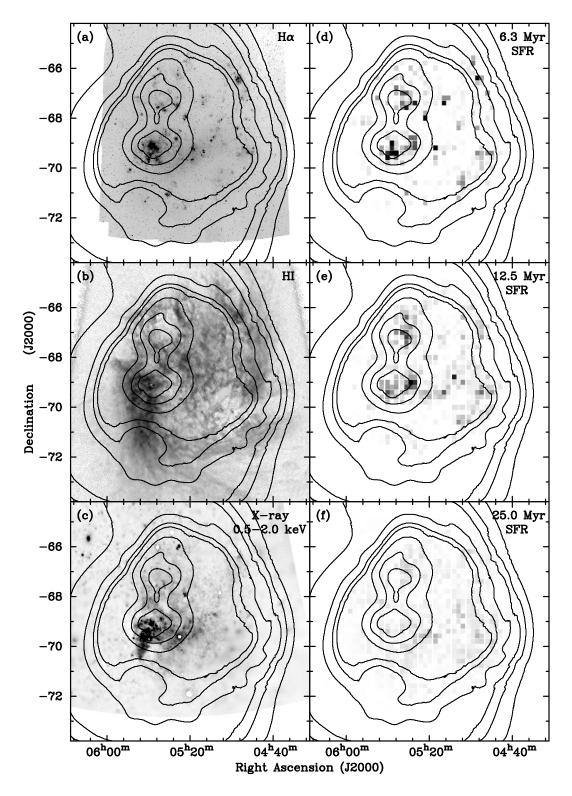
Figure 5: *Fermi* integrated >100 MeV emissivity contours overplotted on (a) MCELS Hα image, (b) H I column density map from Kim et al. (2003), (c) *ROSAT* PSPC mosaic in 0.5-2.0 keV made by S. Snowden, (d-f) maps of star formation rate at ages of 6.3, 12.5, and 25 Myr from Harris & Zaritsky (2009). The Hα, H I, and *ROSAT* X-ray images have been re-cast to the same projection scheme as the *Fermi* emissivity map and the star formation rate maps. The 30 Dor giant H II region is near the brightest γ-ray peak.
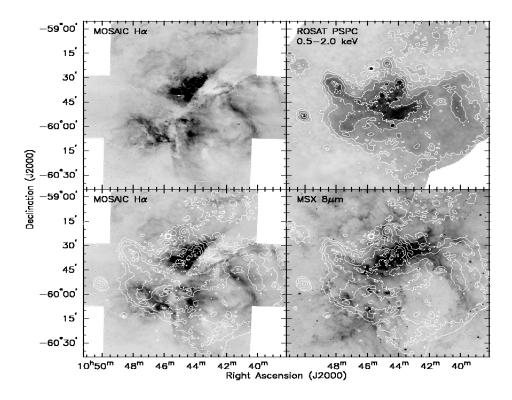
Figure 6: The top left panel shows the Hα emission from the Carina Nebula imaged using the MO-SAIC II camera on the CTIO Blanco 4m. The top right panel shows the X-ray emission in the 0.5-2.0 keV band as seen by the *ROSAT* PSPC (courtesy S. Snowden). The bottom left panel shows the *ROSAT* X-ray emission contours overlaid on the Hα image, while the bottom right panel shows the X-ray contours overlaid on the *MSX* observations at 8μm.

as well as one of the most massive luminous blue variable, η Car (e.g., Walborn 1971; Walborn et al. 2002). As shown in Figure 6, the Hα image of the Carina Nebula reveals non-uniform extinction over the face of the H II region, particularly the V-shaped dust lane running through its waist.

Ever since the first detection of X-ray emission by the *Einstein X-ray Observatory* (Seward & Chlebowski 1982), the nature of the energy source has been debated. An O5 star with $L_w \sim 10^{35}$ ergs s^{-1} injects 2×10^{49} ergs into the ambient ISM during its 5 Myr lifetime, and a WR star can inject 2×10^{50} ergs during 0.5 Myr. A supernova can deposit $10^{50} - 10^{52}$ ergs of explosion energy into the ISM. Thus, both fast stellar winds and supernovae could be important energy sources for the ISM in the Carina Nebula. Based on the absence of nonthermal radio emission and the presence of massive stars with powerful stellar winds, Seward & Chlebowski (1982) suggested that the hot, X-ray-emitting gas is powered by the stellar winds. The only evidence for recent supernovae are an anomalously high column density ratio of N(Mn)/N(Fe) observed toward HD 93205 in the Tr 16 cluster at the heart of the Carina Nebula (Laurent et al. 1982) and the recent discovery of a neutron star candidate in the region (Hamaguchi et al. 2009).

The *ROSAT* PSPC X-ray image of the Carina Nebula (Figure 6) shows diffuse emission in the vicinity of the cluster Tr16, roughly along the V-shaped dust lane, and extending to the southwest. This diffuse X-ray emission is confirmed by deeper, higher-resolution *Chandra* ACIS-I observations in a recent Msec campaign (Townsley et al. 2010). The southwest extension of the diffuse X-ray emission is coincident with a superbubble revealed by the *MSX* 8 μm image (Figure 6). The 8 μm emission detected by *MSX* suffers much less from the local extinction; thus the *MSX* 8 μm image can reveal the true underlying interstellar structure of the Carina Nebula. A second supershell to the

northeast of Tr16 is also seen in the 8 μm image, but diffuse X-ray emission is detected only near its base where the brightest Hα emission is seen.

Recently, we have obtained high-dispersion spectroscopic observations of the Hα and [N II] lines at positions throughout the Carina Nebula (Figure 7). These observations show line-splitting indicating expansion velocities of $\sim$15–30 km s^{-1} at positions that correspond to the *MSX* cavities and centered on Tr 16. Higher-velocity components with typical blue-shifted velocity offsets up to -180 km s^{-1}, and in a few cases red-shifted velocity offsets up to $+130$ km s^{-1} are observed at some positions in and around the dust lane that bisects the Carina Nebula. The higher velocity components appear to be associated with faint "frothy" emission from clumps with linear sizes as small as 0.05 pc extending over areas up to 1-3 pc. These higher velocity components may result from wind-ablated material from the dense gas along the waist of Carina. A more detailed analysis will be presented in Gruendl et al. (in preparation).

Acknowledgements

References

Abdo, A. A., Ackermann, M., Ajello, M., et al. 2010, A&A, 512, 7

Arthur, S. J. 2008, IAUS, 250, 355

Bamba, A., Ueno, M., Nakajima, H., & Koyama, K. 2004, ApJ, 602, 257

Bell, A. R. 1978, MNRAS, 182, 147

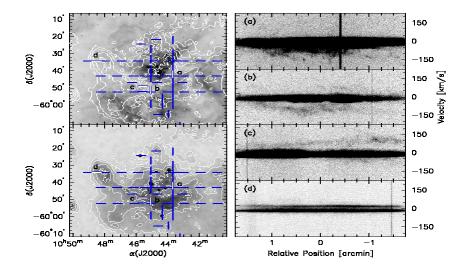Book, L. G., Chu, Y.-H., Gruendl, R. A., & Fukui, Y. 2009, AJ, 137, 3599

Figure 7: (Top Left) An Hα image of the central portion of the Carina Nebula overlaid with contours to show the X-ray emission. The horizontal and vertical marks show the positions of our echelle spectra. (Bottom left) The *ROSAT* PSPC X-ray image in the 0.5–2.0 keV energy band with the same slit positions overlaid. (Right) Each panel shows an echellogram for the [N II] λ6584 emission line. The position of each long-slit is highlighted and marked in the panels to the left.

Bykov, A. M. 2001, Space Science Reviews, 99, 317

Caillault, J.-P., Gagné, M., & Stauffer, J. R. 1994, ApJ, 432, 386

Chen, C.-H. R., Chu, Y.-H., Gruendl, R. A., Gordon, K. D., & Heitsch, F. 2009, ApJ, 695, 511

Chen, C.-H. R., Indebetouw, R., Chu, Y.-H., et al. 2010, ApJ, 721, 1206

Chu, Y.-H. 2008, IAUS, 250, 341

Chu, Y.-H., Guerrero, M. A., Gruendl, R. A., García-Segura, G., & Wendker, H. J. 2003, ApJ, 599, 1189

Chu, Y.-H., & Snowden, S. L. 1998, AN, 319, 101

Cooper, R. L., Guerrero, M. A., Chu, Y.-H., Chem, C.-H. R., Dunne, B. C. 2004, ApJ, 605, 751

Freyer, T., Hensler, G., & Yorke, H. W. 2003, ApJ, 594, 888

Freyer, T., Hensler, G., & Yorke, H. W. 2006, ApJ, 638, 262

Fukui, Y., Kawamura, A., Minamidani, T., et al. 2008, ApJS, 178, 56

Gruendl R. A. & Chu Y.-H. 2009, ApJS, 184, 172

Güdel, M., Briggs, K. R., Montmerle, T., Audard, M., Rebull, L., & Skinner, S. L. 2008, Science, 319, 309

Hamaguchi, K., Corcoran, M. F., Ezoe, Y., et al. 2009, ApJ, 695, L4

Harris, J., & Zaritsky, D. 2009, AJ, 138, 1243

Hughes, A., Wong, T., Ott, J., et al. 2010, MNRAS, 406, 2065

Kawamura, A., Mizuno, Y., Minamidani, T., et al. 2009, ApJS, 184, 1

Kim, S., Staveley-Smith, L., Dopita, M. A. 2003, ApJS, 148, 473

Ku, W. H.-M., & Chanan, G. A. 1979, ApJ, 234, L59

Laurent, C., Paul, J. A., & Pettini, M. 1982, ApJ, 260, 163

Leitherer, C., Schaerer, D., Goldader, J. D. 1999, ApJS, 123, 3

Maddox, L. A., Williams, R. M., Dunne, B. C., & Chu, Y.-H. 2009, ApJ, 699, 911

Meaburn, J. 1980, MNRAS, 192, 365

Meixner, M., Gordon, K. D., Indebetouw, R. 2006, AJ, 132, 2268

Nazé, Y., Chu, Y.-H., Points, S. D., Danforth, C. W., Rosado, M., & Chen, C.-H. R. 2001, AJ, 122, 921

Pittard, J. M., Dyson, J. E., & Hartquist, T. W. 2001, A&A, 367, 1000

Pittard, J. M., Hartquist, T. W., & Dyson, J. E. 2001, A&A, 373, 1043

Puerari, I., Block, D. L., Elmegreen, B. G. & Bournaud, F. 2010, presented at "Galaxies and their Masks" (2010arXiv1008.1044P)

Seale, J. P., Looney, L. W., Chu, Y.-H., et al. 2009, ApJ, 699, 150

Seward, F. D., & Chlebowski, T. 1982, ApJ, 256, 530

Smith, R. C., & the MCELS Team 1999, IAUS, 190, 28

Townsley, L. K., Broos, P. S., Chu, Y.-H., et al. 2010, ApJS, submitted

Vaidya, K., Chu, Y.-H., Gruendl, R. A., Chen, C.-H. R., & Looney, L. W. 2009, ApJ, 707, 1417

Walborn, N. R. 1971, ApJ, 167, L31

Walborn, N. R., Danks, A. C., Vieira, G., & Landsman, W. B. 2002, ApJS, 140, 407

Weaver, R., McCray, R., Castor, J., Shapiro, P., & Moore, R. 1977, ApJ, 218, 377

Wrigge, M., Wendker, H. J., & Wisotzki, L. 1994, A&A, 286, 219

Yamaguchi, H., Sawada, M., & Bamba, A. 2010, ApJ, 715, 412

Yang, C.-C., Gruendl, R.A., Chu, Y.-H., Mac Low, M.-M., & Fukui, Y. 2007, ApJ, 671, 374

Zaritsky, D., Harris, J., Thompson, I. B., & Grebel, E. K. 2004, AJ, 128, 1606

Zinnecker, H., & Yorke, H. W. 2007, ARAA, 45, 481

Discussion

I. Stevens: Can you comment on whether there is any non-thermal X-ray emission in the Carina Nebula?

Y.-H. Chu: There is no obvious diffuse hard X-ray emission of non-thermal origin. It is possible to include a power-low component in the spectral fitting, but that does not necessarily mean the existence of non-thermal X-ray emission.

S. Owocki: I would like to amplify your comment on the role of ablation and mixing in X-ray emission. If the interaction region has turbulent mixing, then the post-shock heated gas mixes with the cooler material and then radiates much more efficiently at UV-EUV- wavelengths, which is hard to detect. I think this could be a key factor in reducing X-ray emission from bubbles, but it's difficult to

quantify because of the unknown level of turbulent mixing in the interaction layer. Perhaps J. Pittard will discuss this further in his talk.

Y.-H. Chu: The 10^5K component cools the fastest. At the interface region and where cool material is mixed into the hot gas, cooling would cause energy loss. This should be considered seriously, but the effects can vary from case to case depending on how much mass-loading has occured.

N. Smith: You mentioned the issue of diffuse X-ray luminosity in giant H II regions being lower than what one expects for a standard wind-blown bubble. It seems probable that one reason for this discrepancy is that H II regions are not necessarily dominated by a pressure-driven stellar wind bubble... Instead it seems likely that radiation pressure and the rocket effect are also very important in driving the expansion of H II regions. As discussed before, mixing and cooling may also help to weaken the X-ray emission.

Y.-H. Chu: This is true in H II regions. There are other objects, such as WR circumstellar bubbles and planetary nebulae, that cannot be explained completely although they have well observed physical properties. Mass-loading from clumps indeed may be very important.

E. Pellegrini: The contribution to the expansion of bubbles due to radiation pressure will be almost equal to the wind energy plus momentum, as seen in a number of high mass star forming regions.

Y.-H. Chu: Well, yes ... in some cases, but it depends on the age and size of the H II region.